14, 119-127 (1968)

MODE DISCRIMINATION OF OPTICAL WAVEGUIDES BY SPATIAL FILTERING*

T. Sawatari, N. S. Kapany and J. J. Burke
Optics Technology, Inc., Palo Alto, California

Abstract

In order to excite only a desired mode, it is sufficient to generate an electro-magnetic field whose transverse components on the end of the fiber match those of the mode. A technique which approximately satisfies this condition is suggested. The results of experiments which involve the use of spatial filtering techniques in the pupil of a launching lens are shown. A method for determining the relative power in each of several modes at the output end of a waveguide will also be presented. It is a vectorial spatial filtering technique, based on the orthogonality of the mode fields. Experimental results confirm the applicability of the method to the one case tested, that of a large diameter optical fiber of low numerical aperture.

Introduction

The optical performance of a straight cylindrical fiber can usually be described in terms of geometrical optics. In this treatment, it is assumed that rays traveling down a fiber are totally internally reflected at the core-coating interface if their angles of incidence at this interface are greater than the critical angle. Thus, the energy associated with these rays is conducted down the length of the fiber. However, if the diameter of the fiber becomes comparable to the wavelength of the light, only certain field distributions (modes) will satisfy Maxwell's equations and the boundary conditions, and in this case, the fiber is more appropriately considered as a waveguide. Even in very large fibers there are waveguide modes, but there are so many of them, their number increases as the area increases, so that a geometrical optics description is generally more fruitful.

Several theoretical and experimental studies of modes have been performed since Snitzer (Ref. 1) first presented the characteristics of modes propagating along the optical waveguide. Kapany and Burke (Ref. 2) investigated the implication of the theory as applied to fiber imaging systems. The radiation characteristics of the modes were also studied by Snitzer (Ref. 3) and Kapany and Burke (Ref. 2). The propagation power of the lower order modes for a plane wave normally incident on the end of a fiber was calculated by Snyder (Ref. 4). In the study of optical waveguides, it is extremely important to find a method (Ref. 5 and 6) where only the desired modes are excited in a waveguide.

In order to excite only the desired mode in a multi-mode guide, it is sufficient to generate an electro-magnetic field whose transverse components on the end of the fiber match those of the mode.

In the first part of this discussion, the use of spatial filtering techniques in the pupil of a launching lens to achieve single mode excitation will be described.

In the second part of this discussion, a method (Ref. 5 and 6) is described which is applicable for the determination of a mode coefficient. The mode coefficient determination method (hereinafter called "mode discrimination method") is introduced by using the orthogonality (Ref. 7) of the mode field. The experimental verification of this method is described by the use of low order modes (HE_{11} and HE_{12}) excited in an optical fiber of large diameter and low numerical

* Supported by the Air Force Office of Scientific Research, Washington, D.C.

aperture.

Waveguide Mode Launching

By generating an electro-magnetic field whose transverse component on the end of the fiber matches those of a desired mode, the desired mode may be excited in a multi-mode guide; however, setting up equations to match the electric and magnetic transverse components generally leads to inconsistent results. This is because the assumed field in a homogeneous half space is only the incident field which has an E/H (ratio of electric field and magnetic field) equal to a constant, whereas the E/H ratio is mode dependent in the guide half space. If the reflected wave is not included, the same relative mode amplitude cannot be obtained from the incident electric field as from the incident magnetic field. Thus, the approach discussed here cannot rigorously give unique self-consistent results. Such results must be obtained through a Green's function approach, where the sources at the end of the fibers are assumed to be the same as those of the incident field with no reaction from the guide. However, if the E/H in a mode can be regarded as an approximate constant, in other words, if only low numerical aperture modes are involved, the above contradiction may be disregarded.

In the following discussion, relatively low numerical aperture modes are treated. Transverse components of the mode field inside the core are given by

$$E_{\pm} \propto J_{n\pm1}(\beta_1 r) e^{i(n\pm1)\phi - hz} \qquad (1)$$

and the components outside the core area

$$E_{\pm} \propto H_{n\pm1}(\beta_2 r) e^{i(n\pm1)\phi - hz} \qquad (2)$$

where J and H are Bessel and Hankel functions of the order of $(n\pm1)$ and β and h are the transverse and axial propagation constants respectively. For the low numerical aperture fibers, the energy propagated along the outside of the core is generally much smaller than that along the inside of the core. Hence, if we can match an incident field to the desired mode field of only the core portion at the entrance end of the fiber $(z = 0)$, only the desired mode will be dominantly excited. Two different methods (Ref. 6) of generating the incident field satisfying the above condition have been assessed theoretically by calculating the mode coefficient which determines the relative amplitude ratio between each mode. As a result, it was found that the use of a spatial filter as the launching lens is one of the simple ways to generate the incident field by which only a desired mode will be excited.

Suppose the function $\frac{\delta(\rho - a')}{a'} e^{in\theta}$ is the distribution in a pupil plane of a lens where (ρ, θ) is a coordinate of the pupil plane, a' is a constant, n is an integer $(0, 1, 2, \ldots)$ and δ is a delta function. The amplitude and phase distribution of the diffraction pattern which is imaged on the entrance end of a fiber will be proportional to the form $J_p(\beta'_1 r)e^{ip\phi}$ in which $\beta'_1 = \frac{2\pi}{\lambda} \frac{a'}{f}$ and f are the forced length of the launching lens. This is shown schematically in Figure 1.

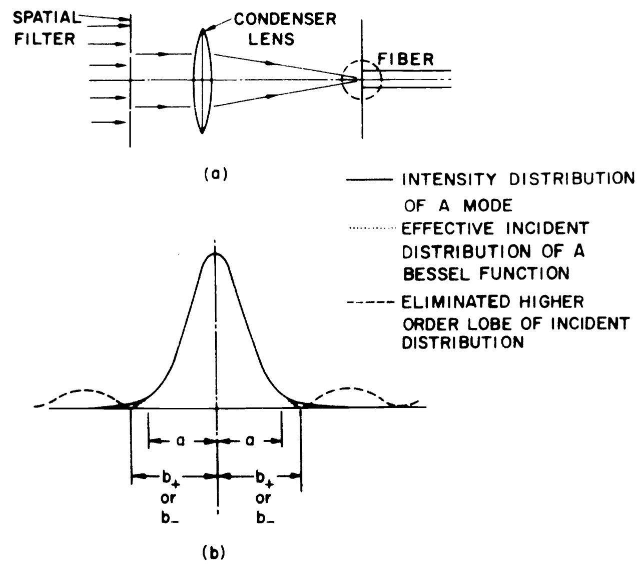

Figure 1. a) Coupling by Spatial Filter; and b) Distribution Generated by a Spatial Filter

****

Therefore, it is experimentally possible to match the field of the diffraction pattern to the desired mode field given in Eq. 1, where β'_1 and p of the incident field must be identical with $(\beta_1$ and $n\pm1)$ of the mode field. Moreover, polarization properties of the incident field must be the same as those of the mode field.

The numerical calculation of the relative power of the mode excited by an incident field has been performed and is listed in Table 1. As is seen in the table, if the parameters β'_1 and p of the diffraction pattern are matched to the desired mode (HE_{11}), the relative power which contributes to excite the desired mode becomes greater than 90 percent and the energy to excite the undesired mode (HE_{12}) becomes less than 0.1 percent of the incident field. (It should be noted that the parameters used in the calculation are $n_1 = 1.53$, $n_2 = 1.52$ and $an_o/\lambda_o = 10.25$, where n_1, n_2 and n_o are the refractive indices of the core, coating and homogeneous half space, a is the diameter of the core and λ_o is the wavelength employed.)

DESIRED MODE	IT'S RELATIVE POWER	UNDESIRED MODE	IT'S RELATIVE POWER
HE_{11}	98.6 %	HE_{12}	0.077 %
HE_{21}	97.6 %	HE_{22}	0.065 %
HE_{12}	95.6 %	HE_{11}	0.080 %
HE_{22}	92.0 %	HE_{21}	0.070 %

Table 1. Relative Power of Waveguide Modes Excited by a Diffraction Pattern of a Spatial Filter

****

Waveguide Mode Discrimination

The orthogonality of optical waveguide mode fields has been shown by Johons in his doctorate thesis (Ref. 7). This orthogonal relation undertakes a significant role in the determination of a mode coefficient of a desired mode in the various modes propagating along a fiber. A vectorial spatial filtering technique, (Ref. 6) based on the performance of the orthogonality in the homogeneous half space, will be analyzed with some approximations, and in the following discussion, modes of a fiber whose numerical aperture is relatively low will be treated.

Consider a large lens placed as shown in Figure 2, where Z_o is the focal length of the lens. Also, assume that the lens has no polarization properties, that is, it is well coated and has no stress and strain so that the electric and magnetic fields in the back focal plate of the lens are obtained from the use of the vector potential concept. Also, it has been shown (Ref. 6) that the far field components are proportional to the Fourier transform of the mode field components, and although rigorously the proportional coefficients are a function of the mode subscripts (n, m), they can be regarded as constants independent of the subscripts for the low numerical aperture fibers under consideration. Furthermore, if another lens is placed at the focal length behind the pupil plane of the first lens, the field in the back focal plane of the second lens (hereinafter called the image plane) is given by the Fourier reverse transform of the field of the pupil plane. Then, it is easily shown that the field components of the image plane are directly proportional to the mode field component given in Eqs. 1 and 2.

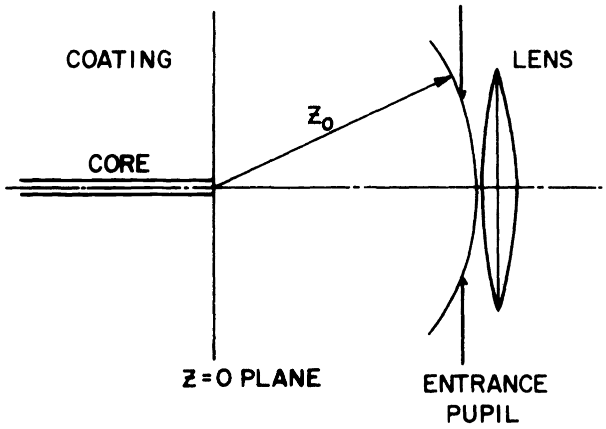

Figure 2. Far Field Wavefront From an Optical Dielectric Waveguide

****

Based on the above mentioned facts, we can discriminate each mode from multi-mode propagating down a fiber as follows. It is known that the mode field in a fiber has an orthogonal relation in the following sense,

$$\int_{\Sigma} (\vec{E}_{tnm} \times \vec{H}^*_{tnm})\vec{Z}d\sigma = C_{nm}\,\delta_{nn'}\,\delta_{mm'} \quad (3)$$

where the integral is performed over a whole cross section (Σ) perpendicular to the Z axis and E_t and H_t are the transverse fields of the mode. C_{nm} is a normalization constant (mode coefficient) and $\delta_{nn'}$ is a Kronkier's δ.

Now, if a similar relation with the orthogonality can be artificially produced in a homogeneous half space by using the far field components discussed above, the mode coefficient C_{nm} may be detected. It should be noted here that in the homogeneous space, the magnetic field is usually proportional to the electric field. Only the electric field will be dealt with in the following discussion.

If the total transverse fields inside the fiber are of the form

$$\vec{E}_t^{tot} = \sum_n \sum_m C_{nm}\vec{E}_{nmt} \tag{4}$$

the electric components of the far field on the pupil plane are then given by

$$e_{\pm}^{'tot} = \sum_n \sum_m C_{nm} e_{nm\pm} \tag{5}$$

where the lower case leter (e) indicates the Fourier transform of the upper case letter (E). Then, consider the following function A

$$A = K_o \int_{\alpha} (e_{+}^{'tot} h_{n'm'+}^{'*} - e_{-}^{'tot} h_{n'm'-}^{'*}) d\alpha \quad (6a)$$

$$A = K_o \sum_n \sum_m C_{nm} \int_{\alpha} (e_{nm+} h_{n'm'+}^{*} - e_{nm-} h_{n'm'-}^{*}) d\alpha \quad (6b)$$

$$= K_o \sum \sum C_{nm} \int_{\Sigma} (E_{nm+} H_{n'm'+}^{*} - E_{nm-} H_{n'm'-}^{*}) d\sigma \quad (6c)$$

$$= K_o \sum \sum C_{nm} N_{nm} \delta_{nn'} \delta_{mm'} \quad (6d)$$

where $H_{n'm'\pm}$ and $h_{n'm'}$ are the artificial functions proportional to the magnetic field components of the mode and the far field respectively, and the star (*) shows the complex conjugate. α is the whole area of the pupil plane and K_o is a constant. The Persival Theorem is used to process Eqs. 6b and 6c. Then from Eq. 3, the resultant Eq. 6d can be obtained.

If the function A can be produced by an experiment, the mode coefficient $C_{n'm'}$ can be obtained with the approximation used. In order to implement the function A experimentally, the arrangement shown in Figure 3 is proposed. A quarter wavelength

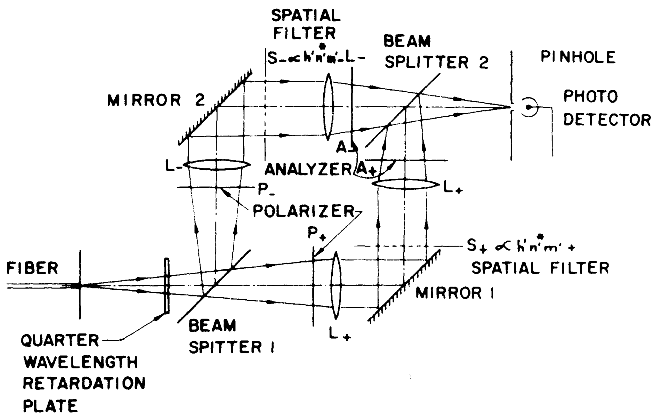

Figure 3. Vectorial Spatial Filtering to Discriminate a Mode From a Multi-Mode Excited in a Fiber

****

retardation plate and polarizers are provided to divide the vector field $\vec{e}$ into each component e_+ and e_-.

Also in Figure 3, P_+ and P_- are the polarizers whose axes have an angle of $\pi/4$ and $-\pi/4$ to the axis of the quarter wavelength plate. Hence, in the back focal plane of the lenses (L_+ and L_-), each field should correspond to the far field component $e_+^{'tot}$ and $e_-^{'tot}$ which are given by Eq. 5. Here each component may be regarded as a scaler field, because their polarization directions have no specific physical meaning. Accordingly, conventional optical filtering techniques may be applied to each path. S_+ and S_- are spatial filters whose amplitude and phase transmittances are proportional to the distribution of $h_{n'm'+}^{'*}$ and $h_{n'm'-}^{'*}$ which are given in Eq. 6a. The subscript (n'm') corresponds to the mode whose coefficient is to be measured. Then, the respective amplitude and phase distribution of the light passing through the filters will be proportional to $e_+^{'tot} h_{n'm'+}^{'*}$ and $e_-^{'tot} h_{n'm'-}^{'*}$ which are included in Eq. 6.

The other two lenses (L_+' and L_-') and the pinhole perform an integral operation of Eq. 6. It is known by the Persival Theorem that the total integral of the amplitude and phase distribution in the pupil plane is proportional to the amplitude on the axis of the image plane. Additionally, the use of analyzers (A_+ and A_-) and the beam splitter (2) produce an interference between the two wavefronts coming from each path. That is, these analyzers, whose axes are parallel to the axis of the quarter wavelength plate, select the coherent portion from the respective fields, for the polarization directions of the fields before the analyzers are mutually perpendicular. Furthermore, it is to be noted that the two paths have π-phase difference to provide the (-) sign in Eq. 6. The intensity measured by a photodetector behind the pinhole will then be proportional to a square of the absolute value of the function A; that is, it will be proportional to $|C_{nm}|^2$.

Experiment

Experimental verification of the above mentioned techniques (mode launching and discrimination) has been carried out for the low order modes (HE_{11} and HE_{12}). In the experiment, fibers of UK50 glass (refractive index = 1.53) coated with a soda lime glass (refractive index = 1.525) were used. Fibers of these materials have essentially no absorption and are of good optical quality. Their low numerical aperture permits the study of waveguide modes of fairly large size (10 microns$\sim$40 microns) and their nonabsorption property provides no mode selection. These fiber properties make them ideal for this study.

The ratio of the diameters of core and coating was approximately 1 to 15. The outer surface of the dielectric coating was coated with black paint to absorb stray light in the coating and the fibers were cemented in capillary tubing (I.D. 1 mm; O.D. 6 mm). The length of the fiber, whose ends were finely polished was approximately 5 cm.

The particular fibers used in this study have a core diameter of 25 microns and can support more than 15 modes at a wavelength of 6328 Å. For fibers of such low numerical aperture, either one of the components (+ or -) of the mode given in Eqs. 1 and 2 becomes much more dominant than the other (- or +), so that the field of low order modes (HE_{11} and HE_{12}) can be considered as a scaler field, e.g., their fields are linearly polarized and the field distribution inside the core is only proportional to $J_o(\beta_1 r)$. This leads to a simplification of the experimental procedure. A schematic diagram of this experiment is shown in Figure 4. The

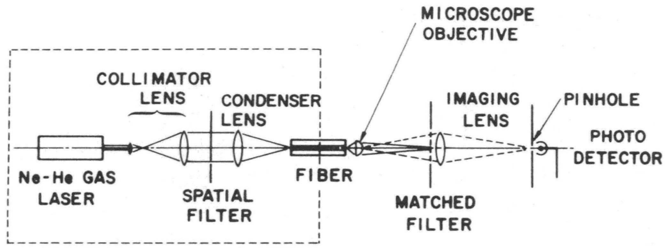

Figure 4. Experimental Arrangement of Mode Launching and Mode Discrimination

****

portion enclosed by dotted lines in the figure is for the mode launching experiment.

A diffraction pattern of a spatial filter (ring aperture) was utilized to excite only the desired mode (HE_{11} or HE_{12}) out of the various possible modes. Photographic methods were used to make the ring aperture. An example of the mask is shown in Figure 5

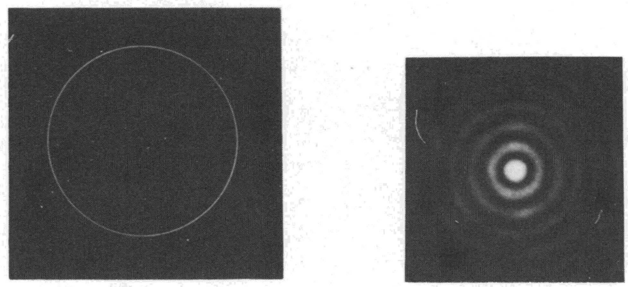

Figure 5. Photograph (Right) of the Diffraction Patterns of a Ring Aperture (Left). These Diffraction Patterns Excite the HE_{11} or HE_{12} Mode in a Fiber

****

compared with the diffraction pattern. The ratio between the diameter and width of the ring was approximately 100 : 1. The diameters of the ring aperture which are calculated to match β'_1 of the incident diffraction patterns to β'_1 of the practical modes (HE_{11}: $\beta_{11} = 1.9 \times 10^2$; HE_{12}: $\beta_{12} = 4.2 \times 10^2$) were approximately 6 and 12 mm respectively where the focal length of the condenser lens was 150 mm.

An He-Ne gas laser, Optics Technology Model 170 Continuous Gas Laser (6328 Å), operating at 0.24 mw single mode output, together with appropriate lenses, was used to make a parallel light beam. Conventional light sources, such as a xenon arc, mercury arc or tungsten source, did not have a high enough intensity, monochromaticy or coherency to produce fine diffraction patterns.

The axis of the fiber was precisely aligned with the axis of the other optical system by using a finely movable fiber supporter. In this adjustment, no auxiliary optics, such as a beam splitter which might introduce a phase disturbance of the light, were used between the lens and the fiber. After this adjustment, the distribution of the light emerging from the exit end of the fiber (near field pattern of a mode) was focused and observed by means of a 50X oil-immersed objective and 10X eyepiece (this procedure is not shown in the figure).

Examples of the desired excited modes (near field pattern of HE_{11} and HE_{12}) are shown in Figures 7a and 8a respectively. The results show the feasibility of this mode launching technique. It should be noted here that the excitation of HE_{11} mode was easier than that of the HE_{12}. The reason for this may be due to the fact that the HE_{11} mode for this fiber was far from cutoff, so that matching of the core portion of the field was quite effective. However, for the HE_{12} mode, the matching of only the core portion was worse.

The portion outside the dotted area in the arrangement shown in Figure 4 is to discriminate each mode propagating down the fibers. The feasibility of this discrimination method is confirmed by the following experimental procedures: 1) a single mode is excited by the launching method discussed above; and 2) for this single mode field, two different mode coefficients are measured, e.g., one is that of the excited single mode and the other is that of another unexcited arbitrary mode. It is then expected that the measured coefficient of the excited single mode will be a finite value and the unexcited mode will be zero.

In the preceding section and as illustrated in Figure 3, a double path method was analyzed theoretically where each path corresponds to each component in the field. However, the condition that the index ratio between the core and coating is close to unity permits a single path operation, because in such a case, as mentioned before, either component (+ or -) becomes negligible. Furthermore, this path operation is performed by using the double diffraction method (Ref. 8) so that the spatial filter is designed to be proportional to the mode field instead of a Fourier transform of the mode field. Here it should be pointed out again that in this case, the dominant components of the low order modes (HE_{11} and HE_{12}) are linearly polarized so that it is not necessary to use the quarter wavelength retardation plate and polarizer. Furthermore, since the diameter of the core is so large and the low order modes in the fiber are far from cutoff, the spatial filters are sufficient as long as the amplitude transmittance is proportional to the Bessel function, because the outside field described by the Hankel function is almost negligible.

The amplitude transmittances of the filters were made on photographic film from the diffraction patterns of ring apertures. The photographic films used were Kodak Panatomic X film (35 mm) for the negative and Kodak commercial sheet film for the positive. The total gamma of these films was controlled to be unity by choosing a suitable time-temperature developing process using Kodal Microdol and Kodak DK-50.

An example of the intensity transmittance of a filter, which was used to discriminate the HE_{11} mode (hereinafter called HE_{11} filter), is shown in Figure 6a with a comparison of the theoretical curve $J_o^2(x)$. Figure 6b is a photograph of another filter used to determine the HE_{12} mode (hereinafter called HE_{12} filter). In order to make the negative portion of the Bessel function in the HE_{12} filter, it was necessary to retard the phase of the outer ring portion by an amount equal to π from that of the central circular portion. This was performed by using a glass plate (microscope slide) having a circular hole in the center. Figure 6c shows an example of the glass plates, where the phase retardation effect is displayed by the interference fringes of a Mach-Zender interferometer.

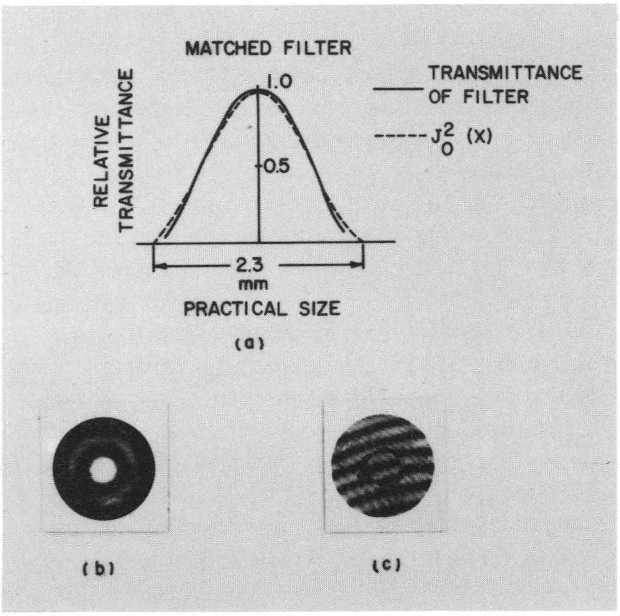

Figure 6. a) Relative Transmittance of a Spatial Filter (for HE_{11} Mode); b) A Photograph of a Filter to Discriminate HE_{12} Mode; and c) Interference Fringes Showing π-Phase Difference of a Phase Plate Attached to HE_{12} Filter

****

In order to eliminate the radiating field from the coating portion of the fiber, a black painted metal plate, which has a hole corresponding to the size of the spatial filter, is placed at the filtering plane (that is, the image plane of the microscope objective).

The intensity on the optical axis at the final plane was measured with a photodetector (EMI 9558B) covered with a pinhole diameter of 20 microns. The intensity was proportional to the square of the desired mode coefficient.

The results of the experiment are shown in Figures 7 and 8 where Figures 7a and 8a are the single modes (HE_{11} and HE_{12}) excited by the "launching method". Figure 7b shows a photograph taken at the image plane of the imaging lens using the HE_{11} filter as a spatial filter. Figure 7b' is a photometric trace of the pattern using a photomultiplier tube to scan the pinhole. A similarly obtained pattern and photometric trace are shown in Figures 7c and 7c', where a spatial filter matching the HE_{12} mode was used for the HE_{11} mode.

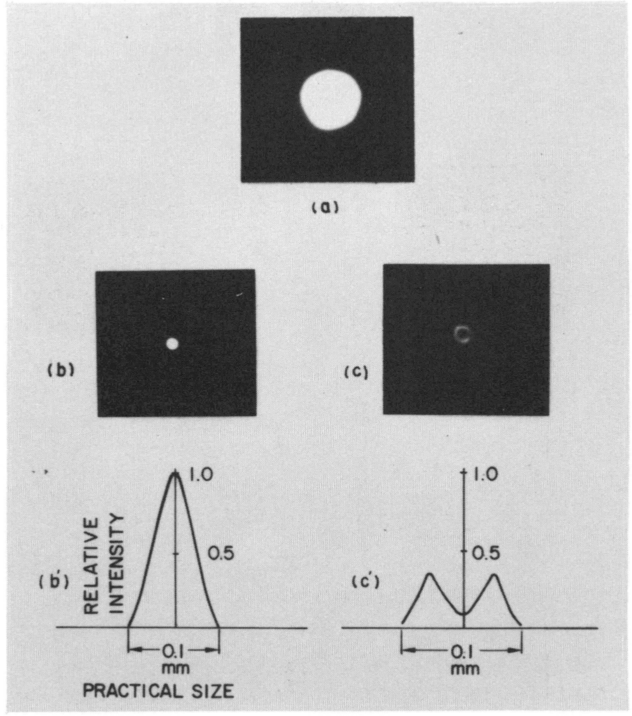

Figure 7. a) HE_{11} Mode Excited in 25-Micron Fiber by a Diffraction Pattern of a Ring Aperture; b) and b') Photograph and Photometric Trace of a Pattern in an Image Plane of a Filtering Lens Where the Filter is Matched to the HE_{11} Mode; and c) and c') Photograph and Photometric Trace of a Pattern in the Same Plane Where the Filter is Matched to the HE_{12} Mode (Which is not Excited in the Tested Fiber)

****

Likewise, Figures 8b and 8b' show a pattern and photometric trace obtained using an HE_{11} filter in the HE_{12} mode. Figures 8c and 8c' show a pattern and photometric trace using an HE_{12} filter in the same HE_{12} mode. These photometric traces can be plotted by taking into consideration the normalization constant N_{lm} (given in Eq. 6d) which is a function of the filter relative amplitude transmittance. Finally, the square of the absolute value of the mode coefficient corresponds to the central value of the photometric traces shown in Figures 7 and 8. The results are shown in Table 2 where the coefficients are normalized by those of the modes initially excited in the fiber.

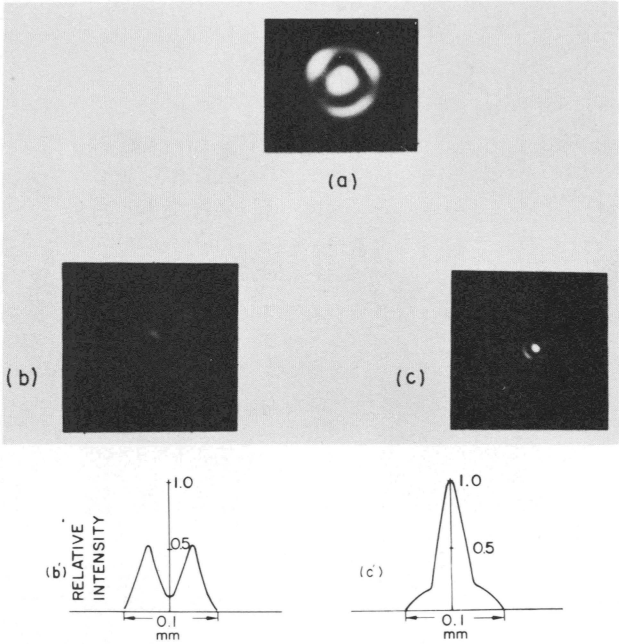

Figure 8. a) HE_{12} Mode Excited in 25-Micron Fiber by a Diffraction Pattern of a Ring Aperture; b) and b') Photograph and Photometric Trace of a Pattern in the Observation Plane Where the Filter is Matched to the HE_{11} Mode (Which is not Excited in the Tested Fiber); and c) and c') Photograph and Photometric Trace of a Pattern in the Same Plane Where the Filter is Matched to the Excited HE_{12} Mode

****

MODE EXCITED IN A FIBER	FORM OF THE FILTER	MODE COEFFICIENT		RELATIVE POWER	
HE_{11}	HE_{11}	C_{11}^{1}	1.0	$(C_{11}^{1})^2$	1.0
HE_{11}	HE_{12}	C_{12}^{1}	0.26	$(C_{12}^{1})^2$	0.07
HE_{12}	HE_{12}	C_{12}^{2}	1.0	$(C_{12}^{2})^2$	1.0
HE_{12}	HE_{11}	C_{11}^{2}	0.36	$(C_{11}^{2})^2$	0.13

Table 2. Experimental Results: Mode Coefficient of Desired Modes and Undesired Modes

****

Summary

Two fundamental problems of optical waveguides, namely, mode launching and mode discrimination, have been approached theoretically and experimentally. In order to excite only a desired mode in a multimode guide, the diffraction pattern of a ring aperture has been used as the exciting field, and the numerical results have shown the applicability of the method if suitable approximations (Ref. 6) for fibers with a low numerical aperture are used. Experiments carried out for lower order modes (HE_{11} and HE_{12}) have also shown the feasibility of the method, and it should be emphasized that such low order modes have been intentionally excited in fibers of more than 15 microns in diameter. However, due to the use of the ring aperture, most of the source (laser) energy is lost in the process; therefore, a study to efficiently couple the energy from the source into the desired mode will be necessary in applying this method practically. In particular, a design study of improved laser cavities, as well as more effective spatial filters, is strongly suggested.

In the determination of the mode coefficient for a desired mode propagating down a fiber which is also supporting other modes, a method called "vectorial spatial filtering", has been analyzed. The vectorial spatial filtering technique is based on the imposing of an orthogonal relationship of mode fields in a homogeneous half space. Experiments performed for low order modes (HE_{11} and HE_{12}) excited in a low numerical aperture fiber whose diameter is 20 microns have shown expected results, when the mode coefficient of a pre-excited mode was assumed to be unity. The coefficients of the unexcited modes were less than 20 percent. It should be noted here that the experiments have been simplified because of the characteristics of the particular modes in the fibers which were used. The applicability of both "mode launching" and "mode discrimination" methods suggests the possibility of a new optical communication system based on a combination of fiber optics and lasers.

References

1. E. Snitzer, J. Opt. Soc. Am. 51, 481 (1961).

2. N. S. Kapany and J. J. Burke, J. Opt. Soc. Am. 51, 1067 (1961).

3. E. Snitzer, in Advances in Quantum Electronics, J. R. Singer, ed. (Columbia University Press, New York, 1961) p. 348.

4. A. W. Snyder, J. Opt. Soc. Am. 56, 601 (1966).

5. T. Sawatari, J. J. Burke and N. S. Kapany, J. Opt. Soc. Am. 57, 584 (1967) (Abstract FE11).

6. T. Sawatari, Ph.D. Thesis, submitted to Waseda University, Tokyo, Japan, January 1968.

7. A. L. Jones, Ph.D. Thesis, Purdue University, Indiana, 1964.

8. J. Tsujiuchi, Progress in Optics (John Wiley & Sons, Inc., New York, 1963) Vol. II.